IEEE Access
Multidisciplinary | Rapid Review | Open Access Journal

Received 21 March 2024, accepted 9 April 2024, date of publication 15 April 2024, date of current version 22 April 2024.

*Digital Object Identifier 10.1109/ACCESS.2024.3388606*

RESEARCH ARTICLE

# Compact Substrate-Integrated Hexagonal Cavity-Backed Self-Hexaplexing Antenna for Sub-6 GHz Applications

**V. JAYAPRAKASH[1,2], (Graduate Student Member, IEEE), D. S. CHANDU[1], (Member, IEEE), RUSAN KUMAR BARIK[3], (Member, IEEE), AND SLAWOMIR KOZIEL[3,4], (Fellow, IEEE)**

[1]School of Electronics Engineering, VIT-AP University, Amaravati, Andhra Pradesh 522237, India
[2]Sri Vasavi Engineering College, Tadepalligudem, Andhra Pradesh 534101, India
[3]Engineering Optimization and Modeling Center, Reykjavik University, 102 Reykjavik, Iceland
[4]Faculty of Electronics, Telecommunications and Informatics, Gdańsk University of Technology, 80-233 Gdańsk, Poland

Corresponding author: D. S. Chandu (chandu.ds@vitap.ac.in)

This work was supported in part by the Icelandic Research Fund under Grant 2410297, and in part by the National Science Centre of Poland under Grant 2020/37/B/ST7/01448.

**ABSTRACT** A self-multiplexing SIW antenna based on hexagonal SIW cavity is proposed. The structure consists of resonating elements of different sizes, which provide the hexaband operations. The antenna resonates at 5 GHz, 5.17 GHz, 5.32 GHz, 5.53 GHz, 5.62 GHz, and 5.72 GHz by employing different slot lengths between the resonating elements. The antenna geometry is arranged so that independent tuning of individual operating frequencies is possible without affecting the remaining center frequencies. The self-hexaplexing antenna exhibits a port isolation better than 29 dB between the resonating elements with a low frequency ratio of 1.14. The simulated gain of the antenna is 5.32 dBi, 5.68 dBi, 5.41 dBi, 5.91 dBi, 5.43 dBi and 5.14 dBi at the respective operating frequencies. The proposed self-hexaplexer operates in the NR band (n46) therefore being suitable for communication system applications.

**INDEX TERMS** Substrate-integrated waveguide, frequency ratio, isolation, self-hexaplexing antenna, tunability.

## I. INTRODUCTION

Multiband antennas developed for next-generation wireless communication systems capitalize on their advantages such as light weight, cost-effectiveness, and ease of manufacturing. Various antenna designs for quad-band [1], [2], [3], pentaband [4], [5], [6], and hexaband [7] operation have been introduced that exhibit the aforementioned features. However, these designs require additional multiplexing circuitry for selecting specific frequency bands, leading to increased space occupancy. Self-multiplexing antennas are typically employed in wireless transceivers instead of multiband antennas. These antennas ensure better performance compared to multiband antennas, which occupy a smaller footprint and do not require additional multiplexing circuitry. Self-multiplexing substrate integrated waveguide antennas [8], [9] offer several features such as improved port isolation, high efficiency, low cost, and size miniaturization, making them suitable for integration into various communication devices.

Another important specific requirement for self-multiplexing SIW antennas is frequency ratio between the antenna operating frequency bands. Low frequency ratio is beneficial because it enables close allocation of distinct frequency bands within the self-multiplexing antenna operating frequency range. In particular, this allows a more efficient use of available sub-bands by allocating more frequency channels with in the given frequency range. Furthermore, low frequency ratio provides high data rate capacity by using a relatively small frequency range. Multiplexing antennas designed with a low frequency ratio are compact, which is

The associate editor coordinating the review of this manuscript and approving it for publication was Wanchen Yang.

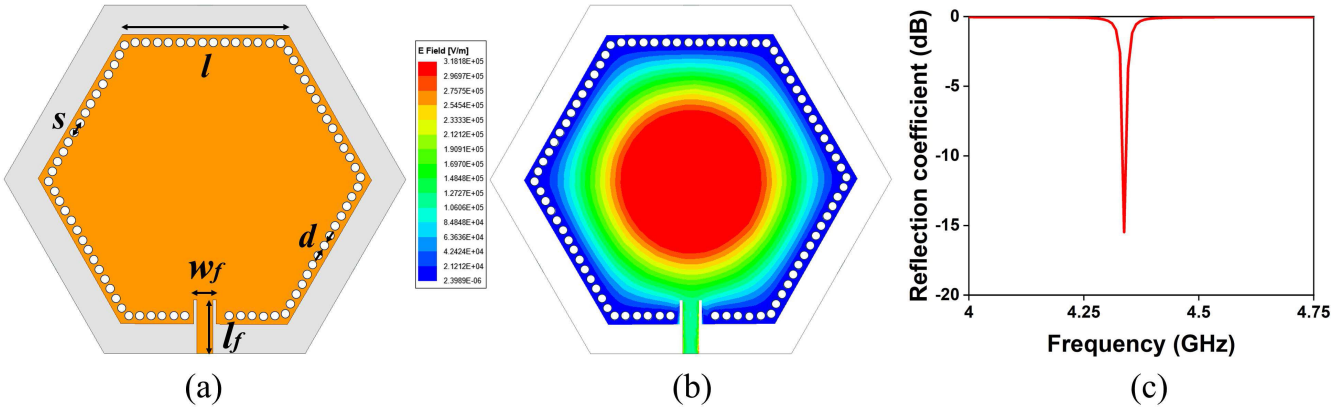


**FIGURE 1.** Geometry of the single port hexagonal SIW resonator [$l = 19.5$, $s = 1.4$, $d = 1$, $l_f = 6.69$, $w_f = 2$ (all are in mm)].

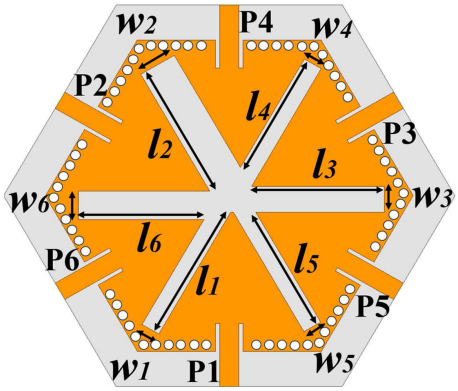


**FIGURE 2.** Schematic-view of the proposed hexaplexing SIW antenna [$l_1 = 14.85$, $l_2 = 14.25$, $l_3 = 13.72$, $l_4 = 13.22$, $l_5 = 13.12$, $l_6 = 13$, $w_1 = 2$, $w_2 = 4$, $w_3 = 1.75$, $w_4 = 2$, $w_5 = 2.5$, $w_6 = 3$ (all are in mm)].

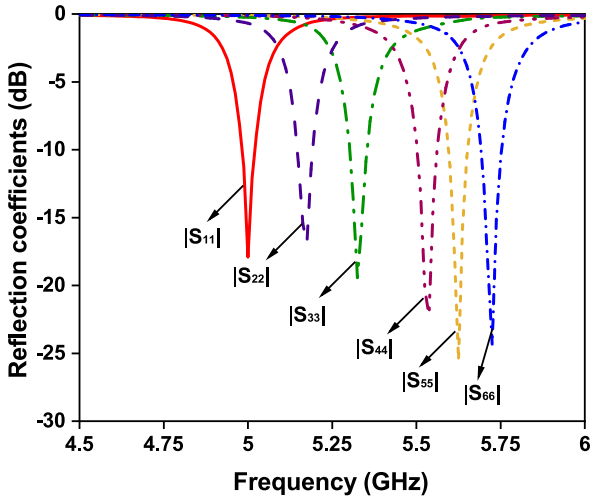


**FIGURE 3.** Reflection coefficient plot of the proposed self-hexaplexing antenna.

desirable in many applications. Another aspect is the sophistication of antenna geometry, which should be preferably low. For example, by utilizing simple slots, the design of a self-multiplexing antenna is less complex and therefore cost-efficient. Several SIW-based self-multiplexing antennas, namely self-diplexers, self-triplexers, self-quadruplexers,

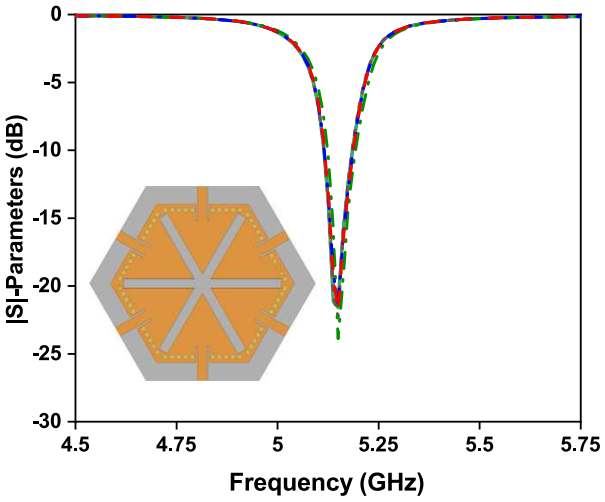


**FIGURE 4.** Reflection coefficient plot of the self-hexaplexing antenna with uniform slot dimensions.

self-quintuplexer, and self-hexaplexers have been developed for dual-band, triple-band, quad-band, penta-band, and hexa-band operation, respectively. The self-diplexing antennas based on bow-tie ring slot [10], rectangular and triangular slots [11], Y-shaped slots and triangular slots [12] have been developed to obtain dual-band operation and achieved significant performance characteristics with a minimum frequency ratio ($f_2/f_1$) of 1.03. A modified I-shaped slot [13], rectangular slots [14], U-shaped slot [15], and two eighth-mode and one quarter mode cavities [16] are employed on different modes of SIW cavity backed antennas such as half-mode SIW cavity (HMSIW), quarter-mode SIW cavity and eighth-mode SIW cavity (EMSIW) and achieved a minimum frequency ratio ($f_3/f_1$) of 1.18 with self-triplexing functionality. Self-quadruplexer antennas have been designed by utilizing different resonating patches [17], U-shaped slots [18], capacitive slots [19], [20], C-shaped and arc-shaped slots [21], and HMSIW with extended resonating slots [22], with a low frequency ratio of 1.34, which is difficult to achieve for a quadruplexing antenna. A self-quintuplexing antenna developed by employing T-shaped and phi-shaped slots [23] obtained a penta-band with a

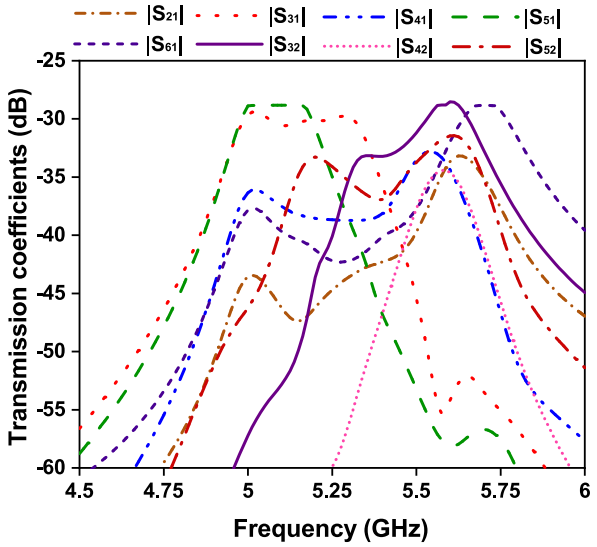


**FIGURE 5.** Transmission coefficients of the hexaplexing antenna.

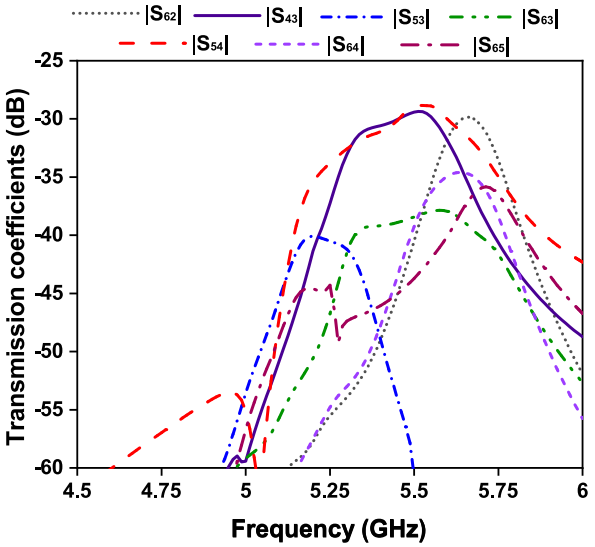


**FIGURE 6.** Transmission coefficients of the hexaplexing antenna.

low frequency ratio of 1.37 between the frequency bands and maintained a significant isolation between the ports. Recently, self-hexaplexing SIW antennas based on two pie-shaped slots [24], rectangular slots [25] and six different patches [26] have been designed. However, design of self-hexaplexing antennas featuring high isolation, low frequency ratio, and high performance in terms of other characteristics is still a significant challenge.

In this study, we propose a self-hexaplexing SIW antenna developed by utilizing different lengths of slots. This approach results in a topologically simple structure with resonant frequencies easy to control by adjusting the slot size. The antenna operates at six resonant frequencies $f_1 = 5$ GHz, $f_2 = 5.17$ GHz, $f_3 = 5.32$ GHz, $f_4 = 5.53$ GHz, $f_5 = 5.62$ GHz, and $f_6 = 5.72$ GHz with a low mutual coupling coefficient not exceeding $-29$ dB. The proposed antenna achieves a low frequency ratio of 1.14 with compact size compared to the state-of-the-art self-multiplexing (triplexer, quadruplexer, quintuplexer, and hexaplexer) antennas reported in the recent literature.

## II. SELF-HEXAPLEXING ANTENNA DESIGN AND ANALYSIS

### A. DESIGN GEOMETRY OF HEXAPLEXING ANTENNA

The hexaplexing SIW antenna is implemented on a Rogers RT/Duroid 5870 with a relative permittivity of 2.33, loss tangent of 0.0012 and a thickness of 0.787 mm. The hexaplexing antenna is designed based on a full-mode hexagonal substrate integrated waveguide (HSIW) cavity resonator as shown in Fig. 1(a). The HSIW is effectively modeled by using the direct approximation of circular substrate integrated waveguide. The resonant frequency of full-mode HSIW [27] is described as

$$f_{mn}^{HSIW} = \frac{c}{2\pi\sqrt{\varepsilon_r}}\frac{k_{c_{mn}}}{l} \tag{1}$$

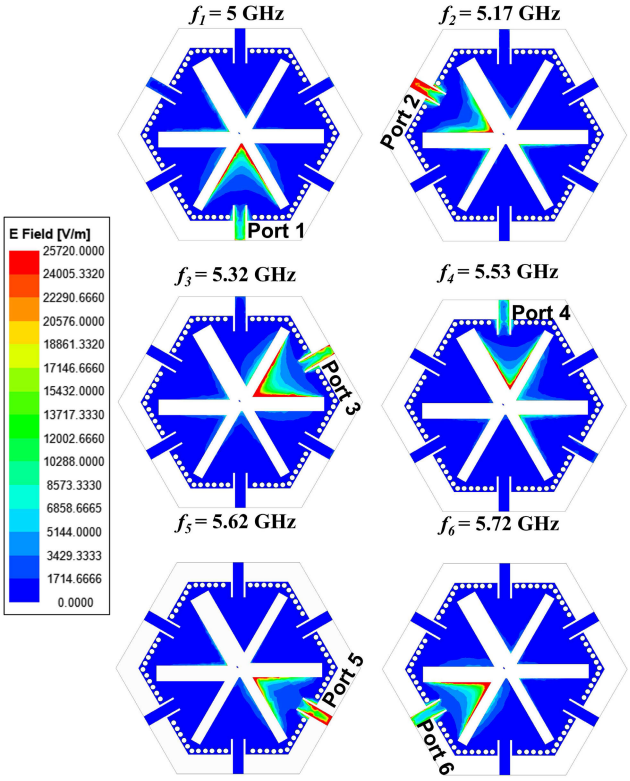


**FIGURE 7.** Electric field distribution at six resonating frequencies.

where, $k_{c_{mn}} = 2.75$ is the cut-off wave number, $c$ is the light velocity in the free space; $\epsilon_r$ is the relative permittivity and, $l$ is the length of the side of the hexagonal SIW. The resonant frequency for $TM_{01}$ mode of operation is given by

$$f_{01}^{HSIW} \approx \frac{2.75c}{2\pi l\sqrt{\varepsilon_r}} \tag{2}$$

The diameter of the via and spacing between the adjacent vias are key parameters that affects the performance of the SIW antenna and must satisfy the condition formulated below

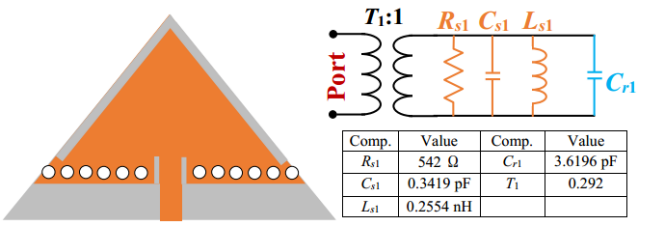


| Comp. | Value | Comp. | Value |
|---|---|---|---|
| $R_{s1}$ | 542 Ω | $C_{r1}$ | 3.6196 pF |
| $C_{s1}$ | 0.3419 pF | $T_1$ | 0.292 |
| $L_{s1}$ | 0.2554 nH | | |

**FIGURE 8.** Equivalent circuit of first resonator associated with Port 1 of the suggested SHA.

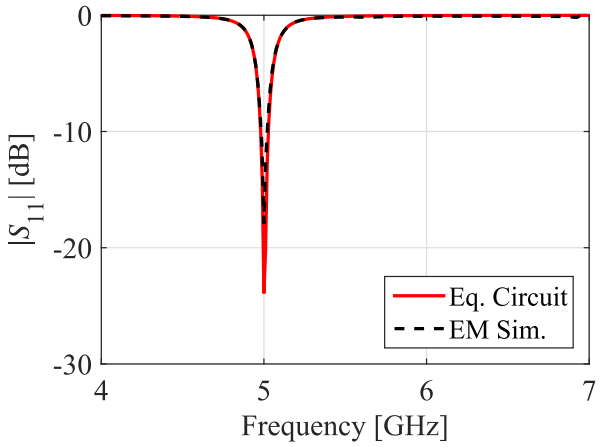


**FIGURE 9.** Circuit and EM simulated reflection coefficient corresponding to port 1.

to reduce the leakage of energy between the vias [8].

$$s \leqslant 2d \tag{3}$$

The electric field distribution of full-mode HSIW is shown in Fig. 1(b). The HSIW with a side length of $l = 19.5$ mm and the fundamental mode of $TM_{01}$ resonates at a frequency of 4.35 GHz, as shown in Fig. 1(c). The hexaplexing antenna is designed by loading different lengths and widths of the slots on a full-mode HSIW antenna by using microstrip feed lines to provide impedance matching, as shown in Fig. 2. The dimensions of slots are optimized in order to achieve a low-frequency ratio, high isolation between the adjacent ports, compact size, and independent frequency tunable characteristics. The separation between the adjacent resonant frequencies is important in order to ensure that the antenna operates within the desired range of frequencies. This can be ensured by the appropriate choice of dimensions of the slots. The hexaplexing antenna operates at six resonant frequencies: $f_1 = 5$ GHz, $f_2 = 5.17$ GHz, $f_3 = 5.32$ GHz, $f_4 = 5.53$ GHz, $f_5 = 5.62$ GHz, and $f_6 = 5.72$ GHz with an electrical size of 0.27 $\lambda_0^2$ as shown in Fig. 3. On the other hand, the influence of slots with the same dimensions on operating frequencies is investigated, as shown in Figure 4. The figure shows that the antenna lacks self-hexaplexing capabilities since all six slots contribute the same operational frequency of 5.15 GHz.

The proposed antenna is designed to operate within the C-band. The existing multiplexing antennas in the literature operate across multiple bands (like S-band, C-band, X-band, etc) that limits their practical applicability. However, operating within a specific frequency band (like only in the C-band as in this manuscript) inherently restricts the available bandwidth. The frequency ratio is defined as the ratio of the upper operating frequency to the lower operating frequency. In the case of a low frequency ratio, the difference between the upper and lower frequencies is small, leading to a narrower bandwidth. As a result of achieving six different frequencies of operation within the available C-band, achieving wide bandwidth and low frequency ratio simultaneously is a not possible. Here, the objective of the manuscript is to achieve independent tuning of frequency bands by achieving high isolation between the ports. Due to this important fact of independent tuning, the resultant 6-port antenna radiates frequencies with narrow bandwidth in all six application bands. The suggested hexaplexing antenna, with its narrow band, could be beneficial for pinpoint applications in commercial wireless applications such as WLAN (at 5.0 GHz), IEEE802.11a WLAN (at 5.25 GHz), WiFi (at 5.4 GHz), and WiMAX (at 5.8 GHz). Moreover, SIW antennas typically exhibit narrow bandwidths at the closely spaced operating bands due to the guided nature of the wave propagation within the substrate. In SIW structures, electromagnetic waves propagate along the substrate integrated waveguide, which confines the electromagnetic fields and limits the frequency range over which the antenna can effectively operate.

The port isolation characteristics between the adjacent antenna elements are shown in Fig.5 and Fig.6. Port isolation better than 29 dB is maintained between any two antenna elements. To gain insight into the performance of the antenna, electric field distributions are plotted at corresponding resonant frequencies. Each port of the antenna can be excited individually, and it can be clearly observed from Fig. 7 that the electric field distribution between the antenna elements is concentrated near the edges of the slots because the conducting surfaces are terminated near the edges of the slots. In any case, although the direction of the current and the relative orientation changes from one port to another, it is worth mentioning that the antenna is linearly polarized.

### B. EQUIVALENT CIRCUIT MODEL OF THE ANTENNA

An equivalent circuit model of cavity-backed resonator corresponding to Port 1 of the suggested self-hexaplexing antenna is shown in Fig. 8. The cavity resonator is modeled as shunt connected resistance ($R_{s1}$), inductance ($L_{s1}$), and Capacitance ($C_{s1}$). The slot associated with the Port 1 is represented by an extra shunt connected capacitance ($C_{r1}$). The slot on the cavity-backed resonator increases the total capacitive loading which allows to achieve smaller footprint by reducing the resonant frequency. The electrical parameter values are determined and shown in Fig. 8. To verify the above concept, the suggested circuit is simulated by using Keysight Advanced Design System (ADS) and the S-parameters are depicted in Fig. 9. In a similar manner, additional ports' analogous circuits may be modeled and verified.

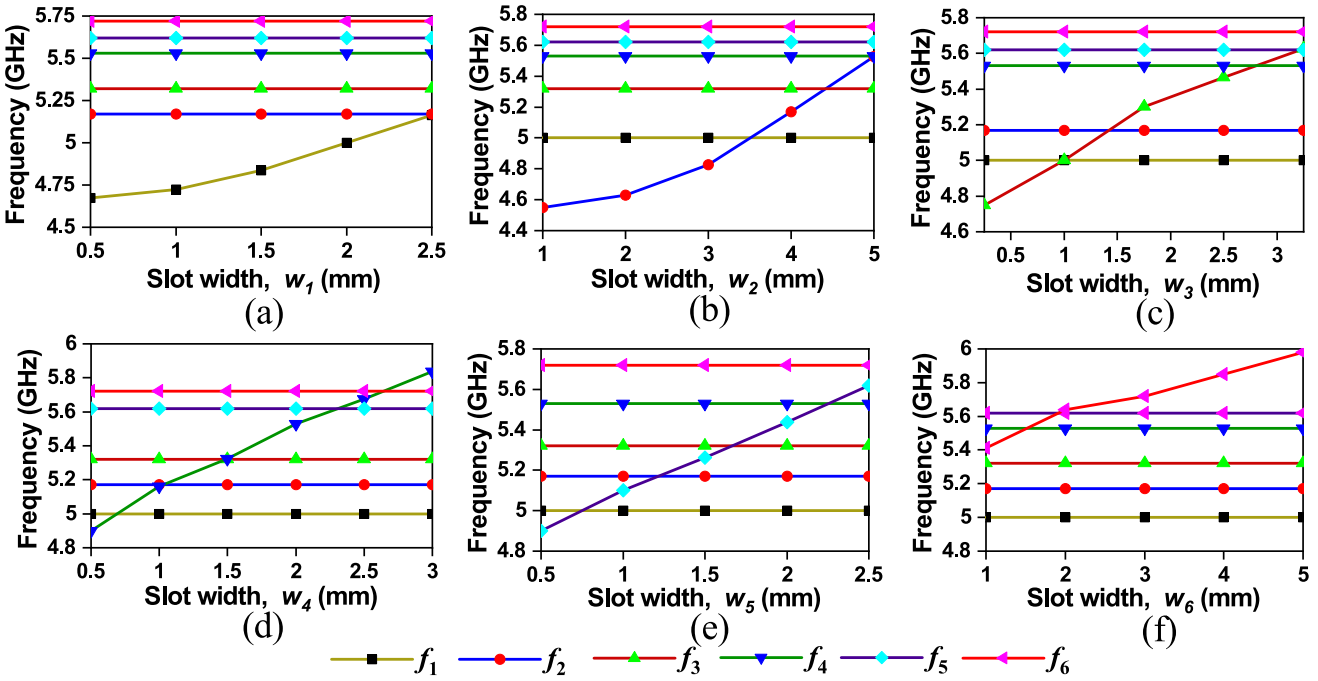


**FIGURE 10.** Individual tunability of the operating frequencies of the hexaplexing antenna.

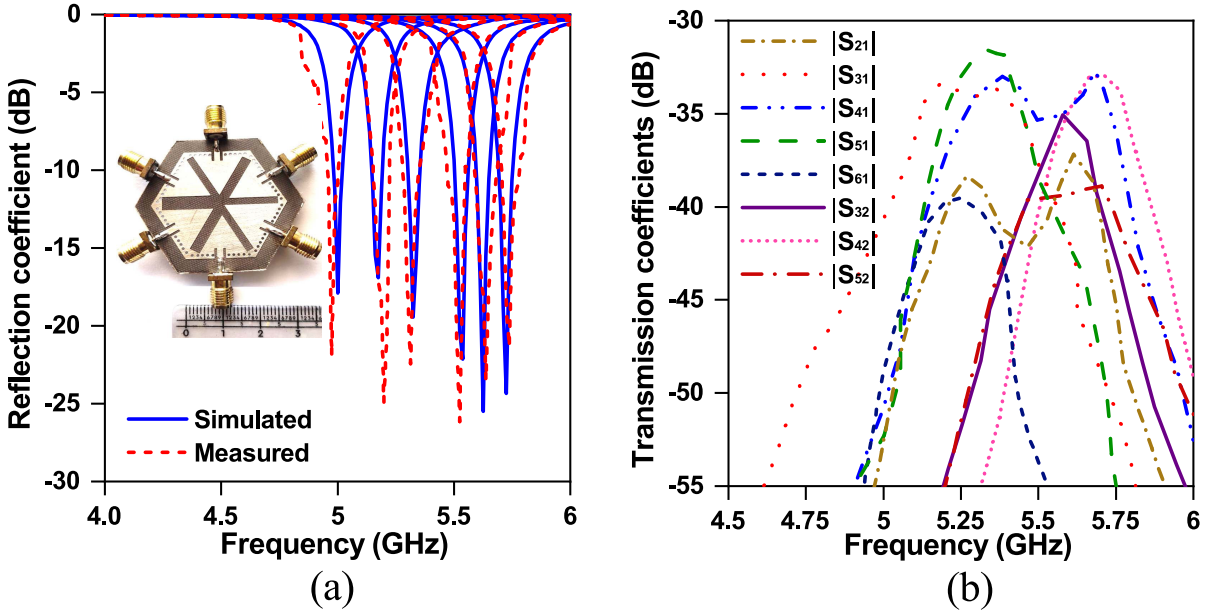


**FIGURE 11.** (a) Photograph of the fabricated prototype of simulated and measured reflection coefficients, (b) measured transmission coefficients of the antenna.

### C. INDEPENDENT FREQUENCY TUNABILITY

The independent frequency tunability of the hexaplexing antenna can be realized by varying the widths of the slots. Fig. 10 (a)-(f) shows the variation of frequency with respect to the design parameters. By varying the width of the slots $w_1$, $w_2$, $w_3$, $w_4$, $w_5$ and $w_6$, a shift the resonant frequencies $f_1$, $f_2$, $f_3$, $f_4$, $f_5$ and $f_6$, respectively, can be obtained. Table 1 shows the independent frequency-tunable characteristics of the hexaplexing antenna by the variation of slot widths. Increasing the width of the slots decreases the resonant frequencies, while decreasing the width increases the corresponding resonant frequencies. This allows the hexaplexing antenna to operate at different frequencies within a desired frequency range. Thus, the ability to adjust the width of slots allows the antenna to cover multiple frequency bands or to operate at different frequencies within a single band, which finds applications in modern communication systems where adaptability to different frequency bands or channels is essential in multi-band communication environments.

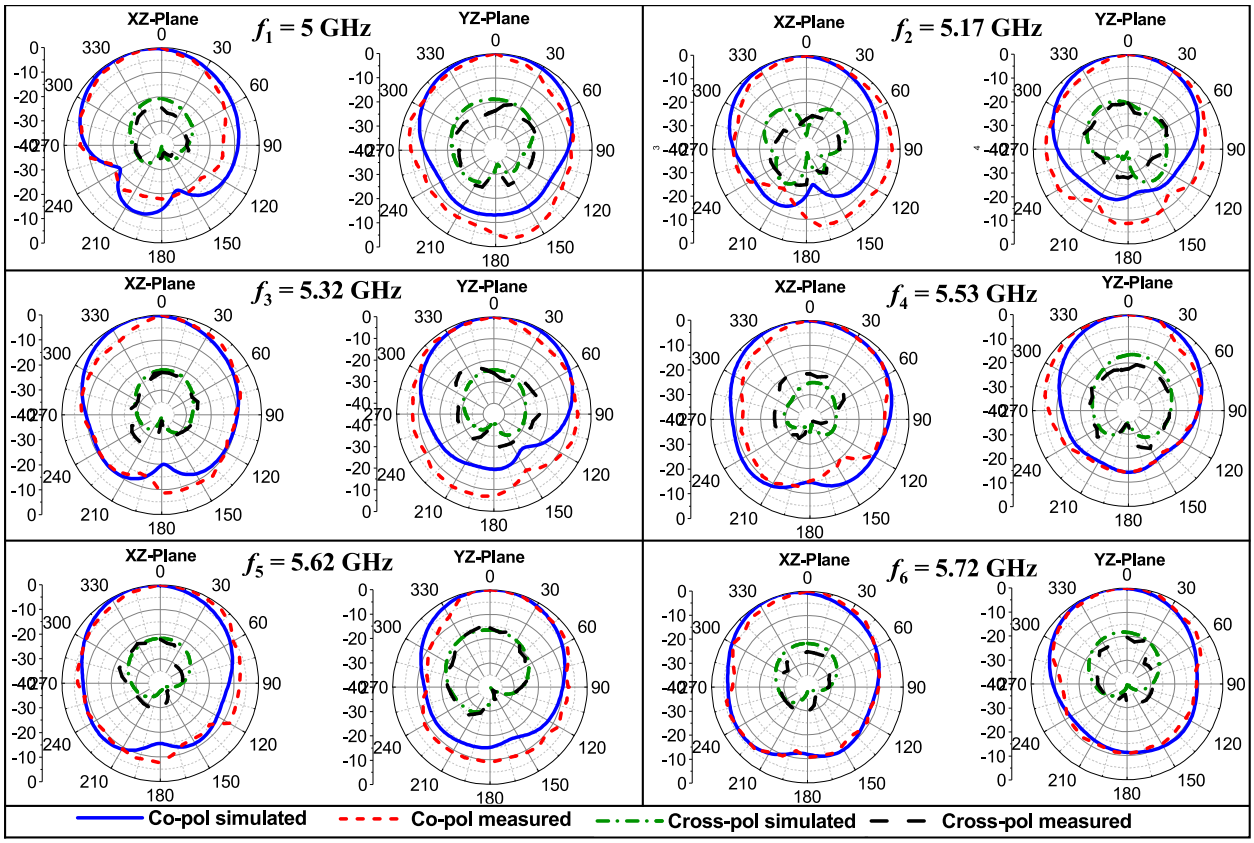


**FIGURE 12.** Simulated and measured normalized radiation pattern in the XZ−plane and YZ−plane.

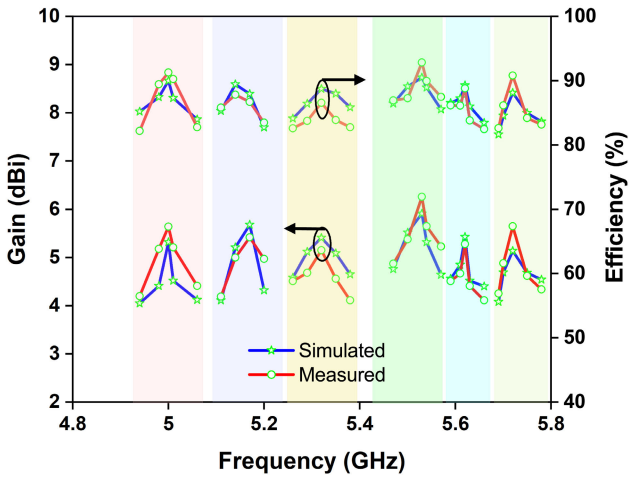


**FIGURE 13.** Simulated and measured gain and efficiency at the six operating frequencies.

## III. RESULTS AND DISCUSSION

The photograph of the fabricated prototype of the hexaplexing antenna based on the aforementioned design specifications is shown in the inset of Fig. 11. The measurements of the reflection coefficient and isolation are performed using Keysight E5063A vector network analyzer. The simulated and measured results for reflection and transmission coefficients of the hexaplexing antenna are shown in Fig. 11(a).

**TABLE 1.** Individual tunable characteristics of the self-hexaplexing SIW antenna.

| Tunable frequency | Variation in slot width (mm) | Variation in frequency (GHz) |
|---|---|---|
| $f_1$ | $w_1 = 0.5$ to 2.5 | 4.67 to 5.16 |
| $f_2$ | $w_2 = 1$ to 5 | 4.55 to 5.25 |
| $f_3$ | $w_3 = 0.25$ to 3.25 | 4.75 to 5.62 |
| $f_4$ | $w_4 = 0.5$ to 3 | 4.9 to 5.83 |
| $f_5$ | $w_5 = 0.5$ to 3 | 4.9 to 5.82 |
| $f_6$ | $w_6 = 1$ to 5 | 5.41 to 5.98 |

The alignment between simulations and measurements is excellent. The measured and simulated isolation is presented in Fig. 10(b) which are very close to each other. There relative discrepancies of between the simulated and measured results are lower than 2%, which may be attributed to manufacturing tolerances. The simulated and measured reflection coefficients are below −15 dB, whereas the transmission coefficients are lower than −29 dB at the corresponding operating frequencies. The simulated and measured normalized radiation patterns in the XZ-plane and YZ-plane are shown in Fig. 12. The patterns are unidirectional in the broadside direction for both planes and the difference between the polarization levels is higher than 20 dB at the respective frequencies because of the SIW structure. Generally, SIW antennas operate based on a waveguide structure integrated within a dielectric substrate. The electromagnetic fields

**TABLE 2. Performance comparison with existing SIW-based multiplexing antennas.**

| Ref | SIW Cavity structure | Frequencies (GHz) | Minimum isolation (dB) | Gain (dBi) | Frequency ratio ($f_h/f_l$)* | Operation |
|---|---|---|---|---|---|---|
| [19] | Square | 5.8, 7.4, 28, 38 | 26 | 4.1, 5.2, 6.1, 8.3 | 6.55 | Quad-band |
| [22] | Square | 4.8, 5.4, 28, 30 | 20 | 5.4, 5.2, 8, 8.7 | 6.25 | Quad-band |
| [18] | Rectangular | 2.33, 2.96, 5.43, 6.15 | 32 | 4.31, 3.39, 6.12, 4.34 | 2.64 | Quad-band |
| [17] | Square | 2.45, 3.5, 4.9, 5.4 | 29 | 3.85, 5.33, 5.95, 5.97 | 2.2 | Quad-band |
| [21] | Circular | 3.5, 4.9, 5.4, 5.8 | 23 | 4.4, 5.07, 5.4, 5.7 | 1.66 | Quad-band |
| [20] | Square | 4.35, 5.35, 5.9, 6.75 | 27 | 4.04, 4.48, 4.55, 6.12 | 1.55 | Quad-band |
| [23] | Rectangular | 2.29, 2.98, 3.65, 4.37, 5.08 | 29 | 3.59, 4.55, 3.91, 5.70, 4.92 | 2.22 | Penta-band |
| [24] | Rectangular | 2.29, 2.96, 4.3, 5.0, 5.61, 6.18 | 27 | 3.73, 4.35, 5.57, 5.46, 4.73 | 2.7 | Hexa-band |
| [25] | Square | 4, 5.8, 6.6, 7.8, 9.8, 10.68 | 27 | 4.9, 5.11, 5.4, 5.43, 5.32, 5.3 | 2.67 | Hexa-band |
| [26] | Rectangular | 5.33, 5.76, 6.31, 6.86, 7.34, 7.8 | 23 | 4.5, 4.94, 4.9, 5.12, 6.12, 6.6 | 1.46 | Hexa-band |
| TW$ | Hexagonal | 5, 5.17, 5.32, 5.53, 5.62, 5.72 | 29 | 5.32, 5.68, 5.41, 5.91, 5.43, 5.14 | 1.14 | Hexa-band |

TW$ = This work, * $f_h$ and $f_l$ are the highest and lowest frequencies, respectively.

in the proposed hexaplexing antenna primarily within the waveguide structure, which is typically formed by metallized vias that are embedded in the dielectric substrate. This confinement of electromagnetic fields within the waveguide of the antenna helps to mitigate the fringing fields and reduces the coupling between orthogonal polarizations. This is one of the reasons behind the reduced cross-polarization of the antenna in the desired direction. The simulated (measured) peak gains are 5.32 dBi (5.64 dBi), 5.68 dBi (5.42 dBi), 5.41 dBi (5.15 dBi), 5.91 dBi (6.26 dBi), 5.43 dBi (5.28 dBi) and 5.14 dBi (5.65 dBi) at the corresponding resonant frequencies of $f_1 = 5$ GHz, $f_2 = 5.17$ GHz, $f_3 = 5.32$ GHz, $f_4 = 5.53$ GHz, $f_5 = 5.62$ GHz and $f_6 = 5.72$ GHz, respectively, as shown in Fig. 13. Similarly, the simulated and measured radiation efficiencies at six bands are $> 80$ % as shown in Fig. 13. During measurements, each port was excited individually with all other ports terminated using the 50Ω load.

The performance comparison of the proposed hexaplexing antenna with the recent state-of-the-art multiplexing antennas has been included in Table 2. The analysis of the performance figures encapsulated in the table demonstrates that the proposed antenna exhibits the lowers frequency ratio of 1.14, while providing comparable gain at the corresponding operating frequencies. Furthermore, the proposed antenna achieved the highest isolation (better than 29 dB) compared to the reported quadruplexing, quintuplexing and hexaplexing antennas. These features make our antenna suitable for communication system applications.

## IV. CONCLUSION

A self-hexaplexing antenna is presented for hexa-band operations, which resonates at six different frequencies. Individual tunability of the frequencies is achieved by varying the selected geometry parameters of the antenna. Full-wave simulations and experimental validation corroborate excellent performance of the proposed structure with port isolation at the lever higher than 29 dB between the antenna elements, and gain better than 5.15 dBi at all operating frequencies. More importantly, the proposed topological arrangement of the antenna results in a low frequency ratio of 1.14, which by far surpasses the capability of the state-of-the-art self-multiplexing antennas reported in the recent literature.

## REFERENCES

[1] M. Martinez-Vazquez, O. Litschke, M. Geissler, D. Heberling, A. M. Martinez-Gonzalez, and D. Sanchez-Hernandez, "Integrated planar multiband antennas for personal communication handsets," *IEEE Trans. Antennas Propag.*, vol. 54, no. 2, pp. 384–391, Feb. 2006.

[2] P. Ciais, R. Staraj, G. Kossiavas, and C. Luxey, "Design of an internal quad-band antenna for mobile phones," *IEEE Microw. Wireless Compon. Lett.*, vol. 14, no. 4, pp. 148–150, Apr. 2004.

[3] D. M. Nashaat, H. A. Elsadek, and H. Ghali, "Single feed compact quad-band PIFA antenna for wireless communication applications," *IEEE Trans. Antennas Propag.*, vol. 53, no. 8, pp. 2631–2635, Aug. 2005.

[4] J. Singh, R. Stephan, and M. A. Hein, "Low-profile penta-band automotive patch antenna using horizontal stacking and corner feeding," *IEEE Access*, vol. 7, pp. 74198–74205, 2019.

[5] K.-L. Wong and C.-H. Huang, "Printed loop antenna with a perpendicular feed for penta-band mobile phone application," *IEEE Trans. Antennas Propag.*, vol. 56, no. 7, pp. 2138–2141, Jul. 2008.

[6] Y. Li, Z. Zhang, Z. Feng, and M. F. Iskander, "Design of penta-band omnidirectional slot antenna with slender columnar structure," *IEEE Trans. Antennas Propag.*, vol. 62, no. 2, pp. 594–601, Feb. 2014.

[7] B. Niu and J. Tan, "Hexa-band SIW cavity antenna system integrating two antennas with high isolation," *Electron. Lett.*, vol. 55, no. 9, pp. 505–506, May 2019.

[8] D. Deslandes and K. Wu, "Accurate modeling, wave mechanisms, and design considerations of a substrate integrated waveguide," *IEEE Trans. Microw. Theory Techn.*, vol. 54, no. 6, pp. 2516–2526, Jun. 2006.

[9] F. Xu and K. Wu, "Guided-wave and leakage characteristics of substrate integrated waveguide," *IEEE Trans. Microw. Theory Techn.*, vol. 53, no. 1, pp. 66–73, Jan. 2005.

[10] R. K. Barik, Q. S. Cheng, S. K. K. Dash, N. C. Pradhan, and K. S. Subramanian, "Design of a compact orthogonal fed self-diplexing bowtie-ring slot antenna based on substrate integrated waveguide," *Int. J. RF Microw. Comput.-Aided Eng.*, vol. 30, no. 11, Nov. 2020.
[11] P. PourMohammadi, H. Naseri, N. Melouki, F. Ahmed, Q. Zheng, A. Iqbal, G. A. E. Vandenbosch, and T. A. Denidni, "Highly-isolated compact self-diplexing antenna," *AEU Int. J. Electron. Commun.*, vol. 173, Jan. 2024, Art. no. 155025.
[12] N. C. Pradhan, S. S. Karthikeyan, R. K. Barik, and Q. S. Cheng, "A novel compact diplexer employing substrate integrated waveguide loaded by triangular slots for C-band application," *J. Electromagn. Waves Appl.*, vol. 36, no. 6, pp. 830–842, Apr. 2022.
[13] S. K. K. Dash, Q. S. Cheng, R. K. Barik, N. C. Pradhan, and K. S. Subramanian, "A compact triple-fed high-isolation SIW-based self-triplexing antenna," *IEEE Antennas Wireless Propag. Lett.*, vol. 19, pp. 766–770, 2020.
[14] P. Nigam, R. Agarwal, A. Muduli, S. Sharma, and A. Pal, "Substrate integrated waveguide based cavity-backed self-triplexing slot antenna for X-ku band applications," *Int. J. RF Microw. Comput.-Aided Eng.*, vol. 30, no. 4, Apr. 2020, Art. no. e22172.
[15] N. C. Pradhan, K. S. Subramanian, R. K. Barik, and S. Koziel, "Shielded HMSIW-based self-triplexing antenna with high isolation for WiFi/WLAN/ISM band," *IEEE Trans. Circuits Syst. II, Exp. Briefs*, vol. 70, no. 6, pp. 1941–1945, Jun. 2022.
[16] V. JayaPrakash and C. Ds, "Self-triplexing HMSIW antenna with enhanced isolation and extremely low frequency ratio," *AEU Int. J. Electron. Commun.*, vol. 170, Oct. 2023, Art. no. 154829.
[17] A. Iqbal, J. J. Tiang, S. K. Wong, S. W. Wong, and N. K. Mallat, "SIW cavity-backed self-quadruplexing antenna for compact RF front ends," *IEEE Antennas Wireless Propag. Lett.*, vol. 20, pp. 562–566, 2021.
[18] R. K. Barik and S. Koziel, "Highly miniaturized self-quadruplexing antenna based on substrate-integrated rectangular cavity," *IEEE Antennas Wireless Propag. Lett.*, vol. 22, pp. 482–486, 2023.
[19] P. PourMohammadi, H. Naseri, N. Melouki, F. Ahmed, A. Iqbal, G. A. E. Vandenbosch, and T. A. Denidni, "Compact SIW-based self-quadruplexing antenna for microwave and mm-wave communications," *IEEE Trans. Circuits Syst. II, Exp. Briefs*, vol. 70, no. 9, pp. 3368–3372, Sep. 2023.
[20] A. Iqbal, M. Al-Hasan, I. B. Mabrouk, and T. A. Denidni, "Highly miniaturized eighth-mode substrate integrated waveguide self-quadruplexing antenna," *IEEE Antennas Wireless Propag. Lett.*, vol. 22, pp. 1–5, 2023.
[21] A. Iqbal, M. Al-Hasan, I. B. Mabrouk, and M. Nedil, "Compact SIW-based self-quadruplexing antenna for wearable transceivers," *IEEE Antennas Wireless Propag. Lett.*, vol. 20, pp. 118–122, 2021.
[22] H. Naseri, P. PourMohammadi, A. Iqbal, A. A. Kishk, and T. A. Denidni, "SIW-based self-quadruplexing antenna for microwave and mm-wave frequencies," *IEEE Antennas Wireless Propag. Lett.*, vol. 21, pp. 1482–1486, 2022.
[23] R. K. Barik and S. Koziel, "Design of compact self-quintuplexing antenna with high-isolation for penta-band applications," *IEEE Access*, vol. 11, pp. 30899–30907, 2023.
[24] R. K. Barik and S. Koziel, "A compact self-hexaplexing antenna implemented on substrate-integrated rectangular cavity for hexa-band applications," *IEEE Trans. Circuits Syst. II, Exp. Briefs*, vol. 70, no. 2, pp. 506–510, Feb. 2023.
[25] N. Melouki, P. PourMohammadi, H. Nasseri, F. Ahmed, A. Iqbal, A. Hocini, and T. A. Denidni, "Ultra-compact quarter-mode SIW self-hexaplexing antenna for C-band and X-band applications," *IEEE Antennas Wireless Propag. Lett.*, vol. 23, no. 3, pp. 995–999, Mar. 2023.
[26] S. K. K. Dash, Q. S. Cheng, R. K. Barik, F. Jiang, N. C. Pradhan, and K. S. Subramanian, "A compact SIW cavity-backed self-multiplexing antenna for hexa-band operation," *IEEE Trans. Antennas Propag.*, vol. 70, no. 3, pp. 2283–2288, Mar. 2022.
[27] S. Banerjee, S. Das Mazumdar, S. Chatterjee, and S. K. Parui, "Half mode semi-hexagonal SIW antennas and arrays for cellular V2X communication," *Microsyst. Technol.*, vol. 27, no. 10, pp. 3639–3651, Oct. 2021.

**V. JAYAPRAKASH** (Graduate Student Member, IEEE) received the Bachelor of Engineering degree in electronics and communication engineering from Jawaharlal Nehru Technological University, Hyderabad, India, the M.Tech. degree in radar and microwave engineering from Andhra University, Visakhapatnam, India, in 2006, and the Ph.D. degree in RF and microwave engineering from Vellore Institute of Technology-Andhra Pradesh University, India. He is currently an Assistant Professor with the Department of Electronics and Communication Engineering, Sri Vasavi Engineering College, Tadepalligudem, Andhra Pradesh, India. His research interests include substrate integrated waveguide antennas, microwave devices, and communication systems.

**D. S. CHANDU** (Member, IEEE) received the B.Tech. degree in electronics and communication engineering and the M.Tech. degree in communication systems from Jawaharlal Nehru Technological University, Hyderabad, India, and the Ph.D. degree in electronics engineering from Indian Institute of Information Technology, India. He was a Faculty Member with the Department of Electronics and Communication Engineering, National Institute of Technology, Andhra Pradesh, India, from 2018 to 2020. He is currently an Assistant Professor with the School of Electronic Engineering, Vellore Institute of Technology-Andhra Pradesh University (VIT-AP University), Andhra Pradesh Campus, India. His research interests include microwave devices, multi-band antennas, and metasurfaces. From 2018 to 2020, he was an Executive Committee Member of the Antennas and Propagation Society of the IEEE Madras Chapter and a Zonal Student Representative of the IEEE Region-10.

**RUSAN KUMAR BARIK** (Member, IEEE) received the B.Tech. degree in electronic and communication engineering from the Biju Patnaik University of Technology, Rourkela, India, in 2012, and the M.Tech. degree in communication systems design and the Ph.D. degree in electronics engineering from Indian Institute of Information Technology, India, in 2015 and 2018, respectively. In 2018, he joined the Department of Electronics and Communication Engineering, Christ University, Bengaluru, India, as an Assistant Professor. In 2019, he joined the Department of Electrical and Electronic Engineering, Southern University of Science and Technology, Shenzhen, China, as a Postdoctoral Researcher. He is currently a Postdoctoral Researcher with the Engineering Optimization and Modeling Center (EOMC), Department of Electrical Engineering, Reykjavik University, Iceland. His research interests include multiband microwave devices, SIW components, surrogate-based modeling, and optimization.

**SLAWOMIR KOZIEL** (Fellow, IEEE) received the M.Sc. and Ph.D. degrees in electronic engineering from Gdańsk University of Technology, Poland, in 1995 and 2000, respectively, and the M.Sc. degree in theoretical physics and the M.Sc. and Ph.D. degrees in mathematics from the University of Gdańsk, Poland, in 2000, 2002, and 2003, respectively. He is currently a Professor with the Department of Engineering, Reykjavik University, Iceland. His research interests include CAD and modeling of microwave and antenna structures, simulation-driven design, surrogate-based optimization, space mapping, circuit theory, analog signal processing, evolutionary computation, and numerical analysis.